

## Biogeochemical cycling in the oligotrophic ocean: Redfield and non-Redfield models

James Robert Christian

Fisheries and Oceans Canada, Canadian Centre for Climate Modelling and Analysis, University of Victoria, P.O. Box 1700 STN CSC, Victoria, British Columbia V8W 2Y2, Canada

### Abstract

The assumption of fixed elemental ratios in ocean biogeochemical models was tested using the Hawaii Ocean Time-Series data set from the subtropical North Pacific Ocean, where nutrient-starvation is a permanent condition for near-surface phytoplankton populations. Two three-element (C, N, P) ecosystem models were coupled to a mixed-layer model, an inorganic carbon chemistry model, and dynamic pools of dissolved organic C, N, and P. One model has fixed Redfield ratios for phytoplankton (constant ratio model, CRM), whereas the other has varying ratios (variable ratio model, VRM). The results suggest that the ecosystem is strongly phosphorus limited, but would be nitrogen limited in the absence of dinitrogen fixation (DNF), and may be nitrogen limited in the lower part of the euphotic zone. Known sources of phosphorus appear to be close to those required to sustain observed levels of export, given plasticity of elemental ratios. The vertical profile and seasonal time course of primary production of organic carbon are simulated well by the VRM but poorly by the CRM, as are surface concentrations of dissolved organic carbon. The seasonal cycles of air–sea CO<sub>2</sub> flux and export of organic carbon by sedimentation are similar in the two models, but there is a slight but persistent bias toward greater downward fluxes in the VRM. The ability of oceanic phytoplankton to adapt to P stress by reducing cellular requirements can therefore potentially enhance the oceanic sink for atmospheric carbon over vast areas of low-latitude ocean, but there is potential for saturation of this enhancement if DNF increases.

The Redfield ratio (RR) is possibly the most robust generalization in ocean biogeochemistry and a cornerstone of the field (Redfield et al. 1963; Sterner and Elser 2002). However, there are systematic deviations from RR whose significance in global biogeochemical cycles remains poorly known. Phytoplankton elemental ratios vary with growth conditions, with the C:N or C:P ratio elevated under nutrient limitation; photosynthesis does not cease in the absence of sufficient nutrients for growth (e.g., Goldman et al. 1979; Geider et al. 1998; Bertilsson et al. 2003). Dissolved organic matter (DOM) appears to be almost universally depleted in N and P relative to the RR (Benner 2002). Many sedimentation data show increasing C:N and C:P in sedimenting particles with increasing depth, implying that remineralization length scales are generally longer for C (e.g.,

Christian et al. 1997). Selective retention of C in the surface ocean by accumulation of C-rich DOM and selective export of C by differential remineralization from sinking particles may occur simultaneously, or one may dominate, depending on location and season.

The subtropical gyres encompass a vast area of ocean ( $\sim 8 \times 10^7$  km<sup>2</sup>) that is for the most part permanently thermally stratified and depleted of nutrients near the surface. The subtropical gyres account for a large fraction of global export, in part because of their sheer size (Karl et al. 1996; Emerson et al. 1997), and phytoplankton production in these nutrient-starved regions is likely to deviate from RR (Goldman et al. 1979; Bertilsson et al. 2003). Nutrient stress will increase the C:N and C:P ratios of primary production, but not necessarily of the standing crop because much of the “excess” C may be lost as exudate (Fogg 1983; Karl et al. 1998; Carlson 2002). Diazotrophy may deplete the upper ocean of phosphorus, giving rise to elevated C:P and N:P ratios while C:N ratios may remain near RR (Karl et al. 1992, 1997, 2001a).

The P cycle in subtropical surface waters is more strongly decoupled from those of C and N than the C and N cycles from each other (Karl et al. 1992, 1997, 2001a). The large variability of N:P ratios and minimal variability of C:N ratios led Emerson et al. (2001) to question the importance of P limitation for C fluxes, as N:P ratios may be so elastic as to permit the export of carbon in proportion to the availability of N. In any case, it is dinitrogen fixation (DNF) that has driven the ecosystem toward a state of P limitation, but even nondiazotrophic phytoplankton can have N:P and C:P ratios significantly in excess of the RR under P limitation (Bertilsson et al. 2003).

The Hawaii Ocean Time-series (HOT) was established in 1988 as part of the U.S. Joint Global Ocean Flux Study program. Since October 1988 approximately monthly cruises

### Acknowledgments

I am indebted to the dedicated team of scientists, students, and technicians who collected and processed the HOT data, and to the vision and leadership of David Karl. James Price provided the source code for his mixed-layer model, and Robert Armstrong his version of the simulated annealing algorithm. Akhil Singh and Jerry Wiggert assisted with development of codes used in this project, and Keith Moore provided useful advice on the implementation of the cellular regulation model. Sergio Signorini developed the original version of the carbon chemistry code. I thank Nick Bates, Andrew Dickson, John Dore, Ernie Lewis, and Rik Wanninkhof for useful discussions about carbon chemistry and air–sea exchange, and Debby Ianson, David Karl, and Sergio Signorini for critical reading of an earlier draft of this manuscript. I am additionally grateful to the National Oceanic and Atmospheric Administration for the NDBC buoy data and to the scientists and agencies responsible for all of the forcing data sets.

This research was supported by the NSF Biological Oceanography program as part of the US-JGOFS Synthesis and Modeling Project.

US-JGOFS contribution 1052.

have measured a wide spectrum of elemental pools and biogeochemical processes. The HOT data set is unique in that both particulate and dissolved organic and inorganic carbon, nitrogen, and phosphorus have been measured consistently throughout its lifetime (the DOC data set does not go back quite to the beginning because of changes in methodology). No other oceanographic program has characterized the complete elemental pools of all three of these elements over an extended period. This data set is therefore an ideal one for testing models of C-N-P stoichiometry and biogeochemistry, because of the length of the time series, the consistency of the methods used, and the completeness of the data.

### Model description

The basic framework of the model is a one-dimensional (depth–time) grid extending from the surface to 500 m with a vertical resolution of 1 m. The physical model is the mixed-layer model of Price et al. (1986). Vertical eddy diffusivity is specified as a bilinear profile with values of  $1.0 \times 10^{-4}$ ,  $3.0 \times 10^{-5}$ , and  $0.5 \times 10^{-5} \text{ m}^2 \text{ s}^{-1}$  at the surface, 250 m and 500 m, respectively; these values were chosen to approximate the profiles estimated by Christian et al. (1997). The model's diffusion subroutine was modified to conserve tracer mass under nonconstant vertical diffusivity. The model was run with a time step of 1 h, resulting in Courant stability limits (Press et al. 1992) of  $1.38 \times 10^{-4} \text{ m}^2 \text{ s}^{-1}$  for diffusivity and  $24 \text{ m d}^{-1}$  for advection or sedimentation velocity.

The model was forced at the ocean surface with wind stress measured at National Data Buoy Center (NDBC) Buoy 51001 (23°24'N, 162°16'W, ~480 km from Station ALOHA) with a constant drag coefficient of 0.0014. These data have been collected on an hourly basis since 1981. Heat fluxes were calculated according to Gill (1982); modeled sea surface temperature was used in all heat flux calculations. Air temperature and barometric pressure from the NDBC buoy was used in these calculations; specific humidity was taken from the National Centers for Environmental Prediction (NCEP) reanalysis (Kalnay et al. 1996). Surface solar irradiance was taken from the International Satellite Cloud Climatology Project (ISCCP) product created by Jim Bishop (Bishop et al. 1997). Daily data are available for 1983–1993, from which a climatology was created; in interannual simulations climatology was used where actual values were unavailable. The diel cycle of irradiance was calculated according to Kirk (1994). Solar irradiance was divided equally between photosynthetically active radiation, with a constant attenuation coefficient of  $0.04 \text{ m}^{-1}$ , and infrared, which is absorbed entirely in the first 1 m. Precipitation was taken from the NASA Global Precipitation Climatology Project (Huffman et al. 1997); precipitation rates were adjusted by constant factor to keep an approximate balance between evaporation and precipitation, as evaporation significantly exceeds precipitation at this location. This data set covers the period 1979–2000. Atmospheric  $\text{CO}_2$  concentrations were obtained from the continuous monitoring program at Mauna Loa, Hawaii (Keeling et al. 1976). Monthly data sets were interpolated linearly to the model time step.

*Biogeochemical model*—Three-element (C, N, P) models were constructed, with fixed (Redfield) ratios for phytoplankton (constant ratio model, CRM) or with varying ratios (variable ratio model, VRM). The biogeochemical model variables are phytoplankton; zooplankton; dissolved organic and inorganic carbon, nitrogen, and phosphorus; and dissolved oxygen. DOM pools are divided into “fast” (labile) and “slow” (semilabile) pools with turnover times on the order of 1 d and 1 yr, respectively (cf. Christian and Anderson 2002). In the CRM, the phytoplankton growth model is a standard photosynthesis–irradiance curve multiplied by a nutrient-limitation term that is the minimum of hyperbolic functions for N and P limitation. Chlorophyll is calculated diagnostically using a light and nutrient concentration-dependent carbon-to-chlorophyll ratio, and phytoplankton and zooplankton are in units of phosphorus with C and N pools implicit. The VRM is based on the model of Geider et al. (1998), with variable internal cell quotas for N and P. Phytoplankton carbon, nitrogen, phosphorus, and chlorophyll are all prognostic variables; zooplankton are assumed to have fixed (Redfield) ratios. The maximum cell quotas for N and P are in RR, whereas the minimum P cell quota is less than the Redfield equivalent (1/16) of the minimum N cell quota, implying that the transition from N to P limitation actually occurs at an N:P ratio considerably higher than the RR (Terry et al. 1985). A simple light-dependent parameterization of DNF adds labile organic N to the surface ocean at a rate that is maximal in summer and at depths of 20–30 m. A complete model description is given in Web Appendix 1 at [http://www.aslo.org/lo/toc/vol\\_50/issue\\_2/0646a1.pdf](http://www.aslo.org/lo/toc/vol_50/issue_2/0646a1.pdf). Model parameters are listed in Table 1.

The fugacity of  $\text{CO}_2$  at the air–sea interface was calculated using the solubility formulation of Weiss (1974), following determination of  $\text{CO}_2(\text{aq})$  from the modeled dissolved inorganic carbon (DIC), temperature, and salinity (Signorini et al. 2001). Oxygen solubility was determined according to Weiss (1970). Alkalinity was calculated as a linear function of salinity on the basis of HOT bottle data ( $r = 0.94$ ). Atmospheric  $\text{CO}_2$  observations were corrected for water vapor following Weiss and Price (1980). Air–sea gas exchange was modeled using the formulation of Wanninkhof (1992).

Initial conditions for dissolved organic and inorganic carbon, nitrogen, and phosphorus; dissolved oxygen; and chlorophyll were derived by fitting polynomials (second or third order as appropriate) to all of the observations collected during December and January. Concentrations of dissolved organic species at 500 m were assumed to represent a “background” pool that is inert on the timescales considered here. The “labile” pools were set to zero at initialization. Initial concentrations of phytoplankton and grazers were derived from the mean profile of particulate nitrogen, assuming half of the total is living biomass, divided equally between the two. Biomass and labile DOM have very short turnover times and are not sensitive to initial conditions. In the VRM, phytoplankton elemental ratios were assumed to be in RR at initialization. Modeled concentrations of dissolved species other than labile DOM were continually relaxed back to the initial conditions at the lower boundary and at depths of 120–200 m. The latter is to prevent drift associated with advection of recently ventilated waters and maintain nutrient

Table 1. Ecosystem model parameters.

Symbol	Description	Units	
<b>CRM*:</b>			
$P_{\max}$	Maximum photosynthetic rate	$\text{g C g Chl}^{-1} \text{h}^{-1}$	6.85
$k_{\text{acc}}$	Photoacclimation coefficient	$(\mu\text{mol m}^{-2} \text{s}^{-1})^{-1}$	0.32
$\theta_{\max}$	Maximum chlorophyll-to-carbon ratio	$\text{g Chl}^{-1} \text{g C}^{-1}$	0.0278
<b>VRM:</b>			
$E_a$	Activation energy	$\text{kJ mol}^{-1}$	37.4
$Q_{\min}^{\text{N}}$	Cell minimum N quota	$\text{g N g C}^{-1}$	0.04
$Q_{\max}^{\text{N}}$	Cell maximum N quota	$\text{g N g C}^{-1}$	0.172
$Q_{\min}^{\text{P}}$	Cell minimum P quota	$\text{g P g C}^{-1}$	0.0018
$Q_{\max}^{\text{P}}$	Cell maximum P quota	$\text{g P g C}^{-1}$	0.0238
$V_{\text{ref}}^{\text{N}}$	Reference rate of N uptake	$\text{g N g C}^{-1} \text{d}^{-1}$	0.6
$V_{\text{ref}}^{\text{P}}$	Reference rate of P uptake	$\text{g P g C}^{-1} \text{d}^{-1}$	0.083
$P_{\text{ref}}^{\text{C}}$	Reference rate of photosynthesis	$\text{g C g C}^{-1} \text{d}^{-1}$	3
$k_{\text{xu}}$	Rate coefficient for exudation	$\text{d}^{-1}$	0.8
$k_{\text{dgr}}$	Rate coefficient for chlorophyll degradation	$\text{d}^{-1}$	0.02
$\zeta$	Respiratory cost of biosynthesis	$\text{g C g N}^{-1}$	2
<b>Common:</b>			
$\alpha_{\text{chl}}$	Initial slope of P-E curve	$(\text{g C g Chl}^{-1} \text{h}^{-1}) (\mu\text{mol m}^{-2} \text{s}^{-1})^{-1}$	0.045
$T_{\text{ref}}$	Reference temperature	K	298
$a_{\text{N}}$	Inorganic N uptake parameter	$\text{mmol}^{-1} \text{m}^3$	30
$a_{\text{P}}$	Inorganic P uptake parameter	$\text{mmol}^{-1} \text{m}^3$	30
$m_1$	Nongrazing mortality rate (linear)	$\text{d}^{-1}$	0.05
$m_2$	Nongrazing mortality coefficient (quadratic)	$\text{mmol}^{-1} \text{P m}^3 \text{d}^{-1}$	0.05
$a_{\text{G}}$	Grazing parameter	$(\text{mmol P m}^{-3})^{-1}$	16
$G_{\text{O}}$	Maximum grazing rate parameter†	$\text{d}^{-1}$	48/24
$\lambda$	Assimilation efficiency	n.d.	0.8
$F_{\text{L}}$	Labile fraction of DOM/POM production	n.d.	0.4
$F_{\text{P}}$	Particulate fraction of DOM/POM production	n.d.	0.12
$k_{\text{w}}$	Light attenuation coefficient	$\text{m}^{-1}$	0.044
$k_{\text{f}}$	Coefficient for attenuation of particle flux	$\text{m}^{-1}$	0.00403
$r_{\text{z}}$	Zooplankton specific respiration rate at $T_{\text{ref}}$	$\text{d}^{-1}$	0.05
$r_{\text{x2}\ddagger}$	Labile DOM remineralization rate at $T_{\text{ref}}$	$\text{d}^{-1}$	0.4
$r_{\text{C1}}$	Semilabile DOC remineralization rate at $T_{\text{ref}}$	$\text{d}^{-1}$	0.001
$r_{\text{N1}}$	Semilabile DON remineralization rate at $T_{\text{ref}}$	$\text{d}^{-1}$	0.0025
$r_{\text{P1}}$	Semilabile DOP remineralization rate at $T_{\text{ref}}$	$\text{d}^{-1}$	0.0027
$R_{\text{DNF}}^{\text{max}}$	Maximum rate of dinitrogen fixation	$\text{mmol}^{-1} \text{m}^{-3} \text{d}^{-1}$	0.0146
$\alpha_{\text{DNF}}$	Dinitrogen fixation photoactivation parameter	$\text{mmol}^{-1} \text{m}^{-3} \text{d}^{-1} (\mu\text{mol m}^{-2} \text{s}^{-1})^{-1}$	$1.32 \times 10^{-6}$
$\beta_{\text{DNF}}$	Dinitrogen fixation photoinhibition parameter	$\text{mmol}^{-1} \text{m}^{-3} \text{d}^{-1} (\mu\text{mol m}^{-2} \text{s}^{-1})^{-1}$	$5.27 \times 10^{-7}$
<b>Intermediates</b>			
$G$	Grazing rate	$\text{mmol P m}^{-3} \text{d}^{-1}$	
$R$	Grazer respiration rate	$\text{mmol P m}^{-3} \text{d}^{-1}$	

\* CRM, constant ratio model; VRM, variable ratio model; DOM, dissolved organic matter, POM, particulate organic matter; DOC, dissolved organic carbon; DON, dissolved organic nitrogen; n.d., non-dimensional.

† Common to both models but value differs (first is CRM value).

‡ X = C, N, or P (see equations A20–A22 in Web Appendix 1).

profiles in the upper thermocline as near as possible to their observed values.

## Results

**Hydrography**—The basic hydrography of the model is shown in Fig. 1. Sea surface temperature ranges were 23–27°C, salinity 33.7–35.7, and mixed layer depth 1–100 m. The maximum winter mixing depth only approaches 100 m in about half the years simulated. Mixed layer depth in summer rarely exceeds 30 m; the mixed layer shows strong diurnal shoaling in all seasons. The means and ranges of all

of these fields are reproduced reasonably well by the model. The seasonal cycle of salinity is much stronger in the model than in the observations. A strong trend to increased salinity occurred from 1997 to 2000. This trend is weaker in the model than in the observations but the trend is reproduced ( $r = 0.72$ ).

**Nitrogen and phosphorus fluxes**—The rate of DNF is modeled in a very simple fashion (see Web Appendix 1), so that additional nitrogen is added to the ecosystem to study its biogeochemical effects. The modeled mean rate of DNF is about one-third greater than the estimated annual rate of

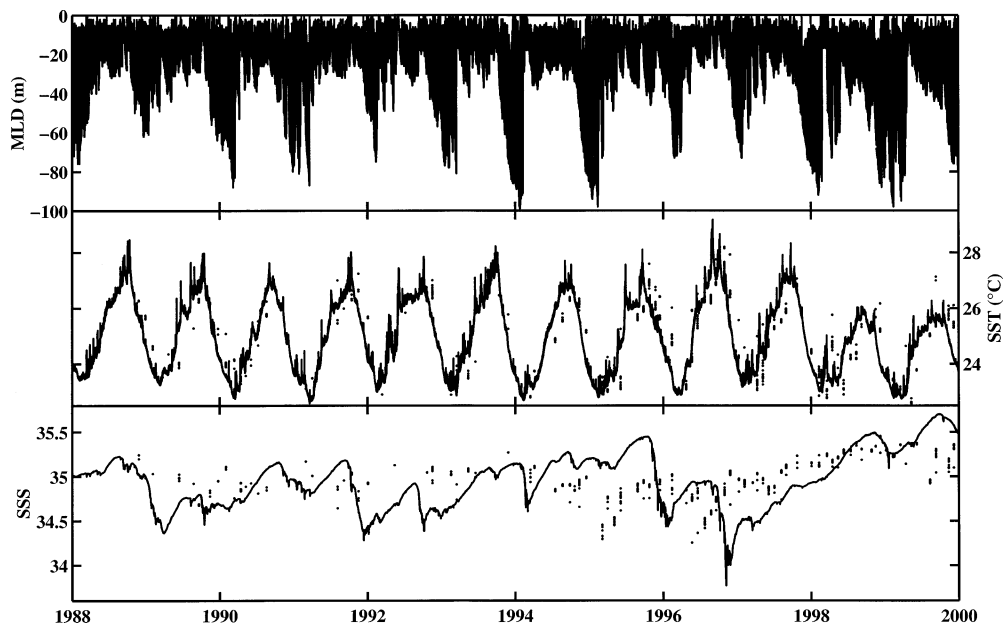


Fig. 1. Time series of mixed-layer depth (MLD) and sea surface temperature (SST) and salinity (SSS) from the mixed-layer model of Price et al. (1986) run with interannual forcing. Solid symbols are observed values from HOT bottle data base for depths less than 5 m. X-axis labels indicate beginning of year.

$\sim 40 \text{ mmol m}^{-2}$  (Karl et al. 1997). Among the key results arising from this experiment are that in the absence of DNF the ecosystem is strongly N limited in both CRM and VRM (Fig. 2), and that with DNF there is an uncontrolled accumulation of dissolved inorganic nitrogen (DIN) in the surface ocean in the CRM (Fig. 3). In the absence of additional

sources of P there appears to be no way to prevent this from occurring in a fixed-ratio model.

An additional possible source of N is atmospheric deposition. Although the rate of deposition of N is not known with certainty, it is considered to be much greater than that of P (Baker et al. 2003). If a flux of N in precipitation (30

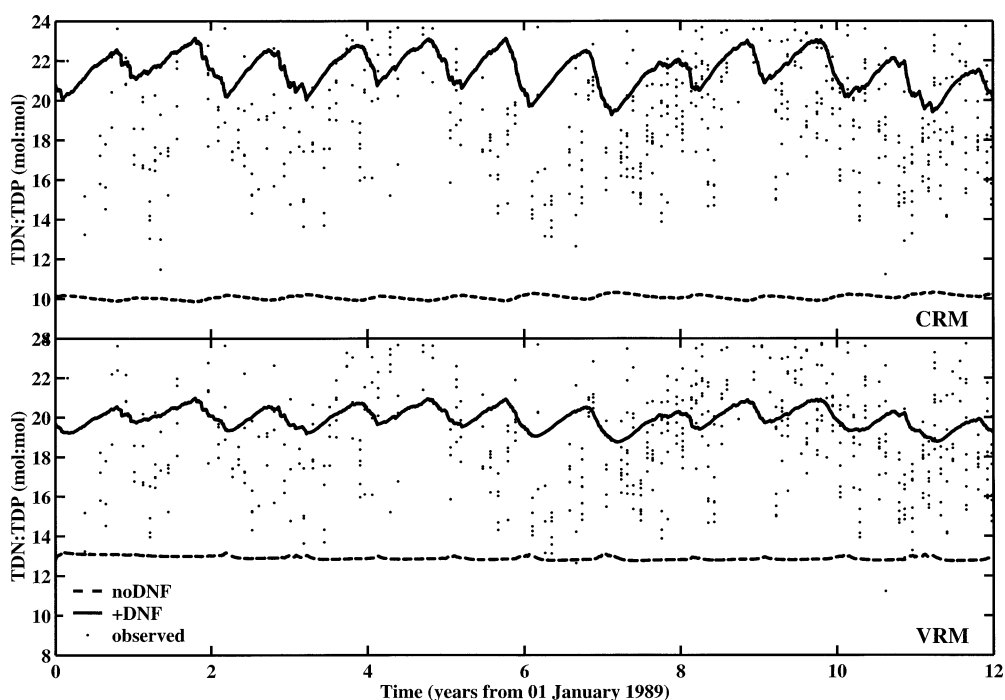


Fig. 2. Surface TDN:TDP ratios in CRM and VRM with and without dinitrogen fixation. Dots are observed values from HOT bottle samples for depths  $< 50 \text{ m}$ .

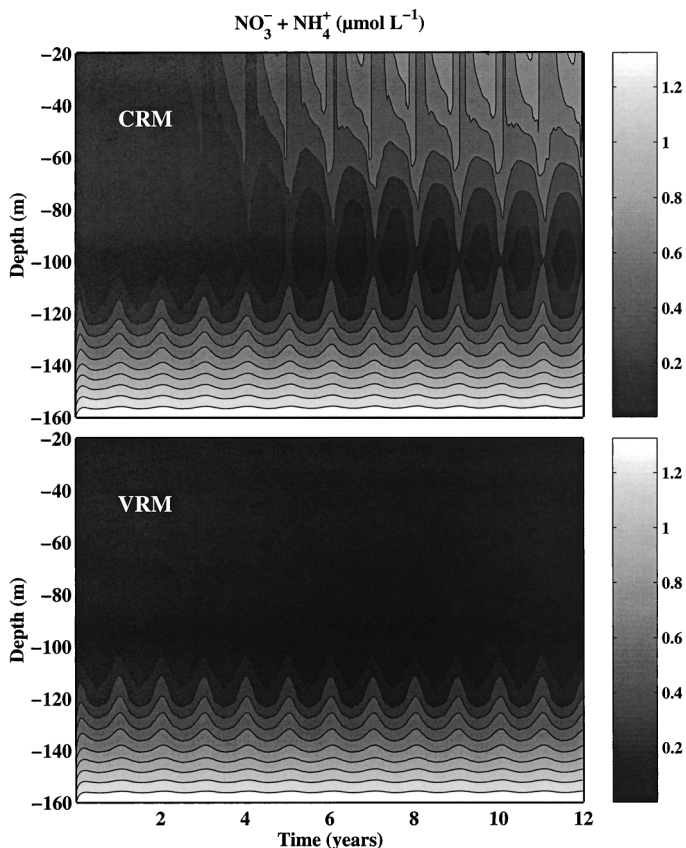


Fig. 3. Depth–time contour plots of DIN in CRM and VRM (12-yr simulation with climatological forcing).

$\mu\text{mol L}^{-1}$  was taken as an upper limit for oceanic regions; Cornell et al. 1995) to the surface of the ocean is included in the model, it has little effect on production, export, or carbon flux, above that induced by  $\text{N}_2$  fixation (Table 2). In the CRM, N is already in excess (Fig. 3). In the VRM, the ecosystem is capable of absorbing some additional N, and small amounts of additional N have a positive effect on primary productivity. However, at high rates of input, DIN accumulation occurs even in the VRM, and in the fully spun-

Table 3. Elemental ratios in phytoplankton biomass (mixed layer) and particle flux (300 m). noDNF indicates values for phytoplankton biomass in a simulation without dinitrogen fixation. Means for 1989–2000.

		Minimum	Maximum	Mean	Median
Particle flux	C:N	6.6	9.0	7.9	7.9
	C:P	106.0	141.4	130.6	130.8
	N:P	14.6	18.7	16.6	16.6
Biomass	C:N	8.0	12.1	9.5	9.2
	C:P	131.2	408.7	312.9	337.3
	N:P	13.7	47.3	33.7	35.7
noDNF	N:N	9.4	16.4	14.3	14.5
	C:P	114.8	168.4	148.8	151.6
	N:P	8.1	14.5	10.4	10.7

up model primary productivity is lower than in the base simulation (Table 2). In the CRM there is no drawdown of DIC when additional atmospheric N deposition is added (except as a transient during the spin up to steady state), whereas in the VRM there is a consistent offset of  $\sim 2 \mu\text{mol L}^{-1}$  (Table 2). So in the CRM atmospheric deposition of N, or elevated rates of DNF, can do little to stimulate production or export of carbon in the absence of additional sources of P.

P limitation in the VRM can potentially be alleviated by increasing the elasticity of cellular elemental ratios, e.g., by reducing the minimum P cell quota ( $Q_{\min}^{\text{P}}$ ). The basic simulation has a lower  $Q_{\min}^{\text{P}}$  for P than N by a factor of 48 on a molar basis (i.e., one-third of the “Redfield equivalent”). Further lowering this quota has little effect on the ecosystem. For a minimum cell quota half the base value or 1/6 of the “Redfield equivalent”, surface DIC decreases by  $<0.1 \mu\text{mol L}^{-1}$  and DIN increases by  $\sim 0.1 \text{ nmol L}^{-1}$  (Table 2). Surface dissolved organic carbon (DOC) increases by  $0.15\text{--}0.20 \mu\text{mol L}^{-1}$ , with the maximum difference in summer (not shown). Primary production of carbon increases by  $1\text{--}2\%$  (Table 2).

C:N:P ratios in phytoplankton in the VRM deviate quite significantly from RR in the surface ocean, whereas sinking fluxes of C, N, and P at 300 m do not (Table 3). The mean modeled sinking fluxes of N and P at 300 m are  $94 \mu\text{mol m}^{-2} \text{ d}^{-1}$  and  $5.8 \mu\text{mol m}^{-2} \text{ d}^{-1}$ , respectively, which are sim-

Table 2. Diagnostics of biogeochemical effects of N sources and minimum P cell quota. Base simulation has dinitrogen fixation (DNF) but no atmospheric deposition, and  $Q_{\min}^{\text{P}} = Q_{\min}^{\text{N}}/48$ . +atmN indicates atmospheric N wet deposition at a concentration of  $30 \mu\text{mol L}^{-1}$  in addition to DNF; no DNF indicates neither DNF nor atmospheric deposition; PQ6 indicates  $Q_{\min}^{\text{P}} = Q_{\min}^{\text{N}}/96$  or half of the base value. Inorganic species concentrations are at the sea surface; PP = depth-integrated primary production in  $\text{mmol m}^{-2} \text{ d}^{-1}$ ; export is of C at 150 m depth in  $\text{mmol m}^{-2} \text{ d}^{-1}$ . All are means for the final year of a 12-yr simulation with climatological forcing.

Model	Simulation	DIC ( $\mu\text{mol L}^{-1}$ )	DIN ( $\text{nmol L}^{-1}$ )	DIP ( $\text{nmol L}^{-1}$ )	Export	PP
CRM	base	1978	696	12	0.99	11.1
	+atmN	1978	2907	12	0.99	11.1
	noDNF	1981	4.4	74	0.79	8.2
VRM	base	1974	1	0.45	1.24	36.1
	+atmN	1972	723	0.46	1.40	28.4
	noDNF	1976	0.3	0.41	1.10	35.7
	PQ6	1974	1.1	0.45	1.25	36.8

\* DIC, dissolved inorganic carbon; DIN, dissolved inorganic nitrogen; DIP, dissolved inorganic phosphorus; CRM, constant ratio model; VRM, variable ratio model.

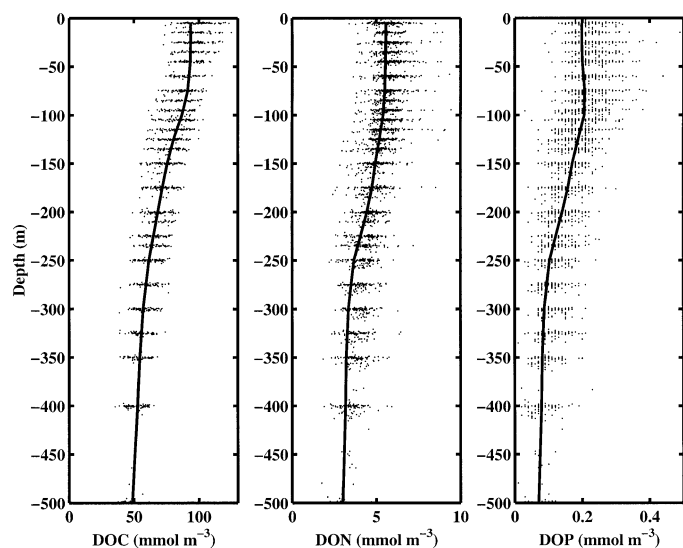


Fig. 4. Vertical profiles of DOC, DON, and DOP. Dots are observed values from HOT bottle samples. Solid lines are modeled values from VRM (mean for final year of 12-yr simulation with climatological forcing).

ilar to the observed fluxes from HOT sediment trap data (Christian et al. 1997). The N:P ratio is very close to the RR, whereas C:N and C:P ratios are slightly elevated relative to the RR (Table 3). Near-surface phytoplankton biomass, by contrast, has C:P and N:P ratios that are two to three times greater than the Redfield ratios (Table 3). These ratios show a distinct seasonal cycle with a maximum in summer (not shown), because both DNF and photosynthesis are maximal during summer while cell production is limited by the availability of phosphorus. In winter (and below the mixed layer), the N:P ratio falls below the RR because of the influx of new inorganic nutrients; the inorganic pool is depleted in N in the lower part of the euphotic zone (Karl et al. 2001b). Values for a simulation without DNF are also shown in Table 3; the N stress on the phytoplankton is illustrated by C:N and N:P ratios that are respectively greater and less than the corresponding Redfield ratios. C:P ratios are also greater than RR, so an elevated C:P ratio is not by itself a definitive diagnostic of P limitation.

**DOM profiles and turnover times**—The vertical profiles of dissolved organic carbon, nitrogen and phosphorus (DOC, DON, DOP) can be reasonably well reproduced by assigning turnover times for the semilabile pools on the order of 1 yr for N and P and 3 yr for C, and temperature-dependent remineralization with a  $Q_{10}$  of 2.6 (Fig. 4, Table 1, see Web Appendix 1). The relative rates for the three elements are based on the observed abundances of the total organic pools; this aspect of the model therefore estimates an important part of the solution directly from the data and sheds little light on mechanisms. A weaker temperature dependence (e.g., a  $Q_{10}$  of 1.5) tends to cause drift in either surface or thermocline values (not shown).

The constraints given by the HOT data set permit an assessment of the turnover times for the dissolved organic pools and the partitioning of production of nonliving matter

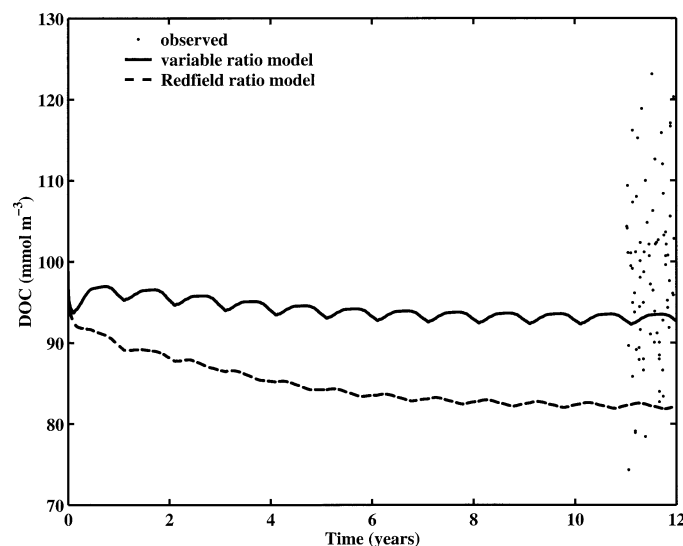


Fig. 5. Time course of surface concentration of DOC in variable ratio model and Redfield ratio model. Twelve-year simulation with climatological forcing; observed values plotted against day-of-year for final year only.

among the various pools. However, these parameters are correlated and can not all be strongly constrained simultaneously, i.e., adjusting two parameters simultaneously could give a more or less equivalent solution, for example, increasing both the fractional production of semilabile DOP and its remineralization rate. The model nonetheless illustrates a self-consistent solution for these parameters, with mean lifetimes at 25°C of about 2.5 d for labile DOM, 1 yr for semilabile DOP and DON, and 2.75 yr for semilabile DOC (Table 1). Loss processes other than exudation (which is assigned exclusively to the labile fraction) produce about 40% labile DOM, 48% semilabile, and 12% sinking particles, i.e., the estimated turnover times are consistent with about half of the flux from the living to the nonliving pools going to semilabile DOM and about 12% to sedimentation. The decoupling of photosynthesis and growth in the VRM produces significant accumulations of phytoplankton carbon, and maintaining the observed concentrations of DIC and DOC (as well as cellular ratios that do not deviate too far from RR) requires that this “excess” carbon be leaked to the dissolved pool and rapidly remineralized (hence the requirement that none of this flux goes to the semilabile pool). In the CRM, by contrast, the concentration of DOC is lower than observed in near-surface waters (Fig. 5). DOC is one of the model variables for which no acceptable parameter set was found that would permit the CRM to reproduce the observations.

**Carbon cycle**—A key carbon-cycle process that shows a stark contrast between the two models is primary production. Seasonality of primary production is weak at Station ALOHA (Fig. 6). Depth-integrated primary production is maximal in summer (Fig. 7), and most primary production occurs in the surface mixed layer (Fig. 6). The decoupling of photosynthesis, chlorophyll synthesis, and cell production in the cellular-regulation model is necessary to achieve a realistic

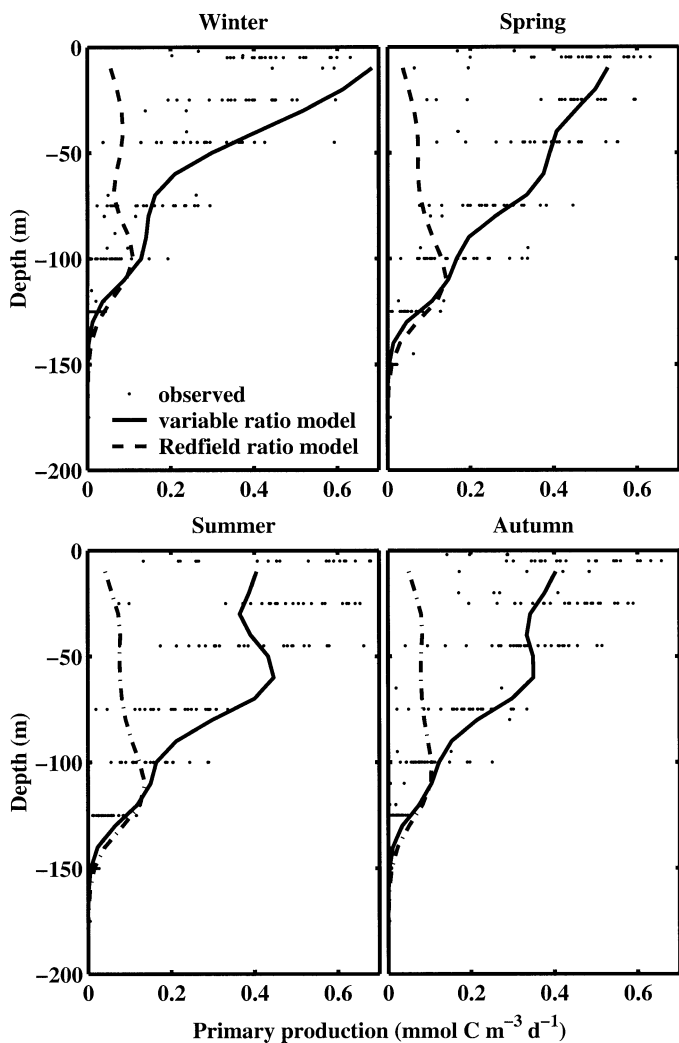


Fig. 6. Vertical profiles of observed and modeled primary production at Station ALOHA.

simulation of these observations (Figs. 6, 7). The seasonal and vertical distribution of  $^{14}\text{C}$  primary production is closely related to ambient solar irradiance, and these patterns are not reproduced in the fixed-ratio model.

The inorganic carbon balance of the surface ocean is determined by air–sea exchange of  $\text{CO}_2$ , vertical mixing, biological uptake and remineralization, and advection; the total carbon balance depends only on sedimentation of particulate carbon and not on biological transformations as such. Fluxes of carbon in and out of the upper 300 m at ALOHA are shown in Fig. 8. For clarity only the VRM results are shown; the CRM has a similar seasonal cycle, but with a small but persistent bias toward smaller downward fluxes (Table 4). At any given time, air–sea exchange is generally the largest term, but the annual mean is similar to the export flux because the flux reverses direction seasonally (Fig. 8; Table 4). The seasonal cycle of surface  $\text{CO}_2$  fugacity ( $f\text{CO}_2$ ) at HOT is much smaller than at the Bermuda Atlantic Time-Series station (BATS, cf. Karl et al. 2001b) and the seasonal reversal less obvious, with an overall bias in favor of flux into

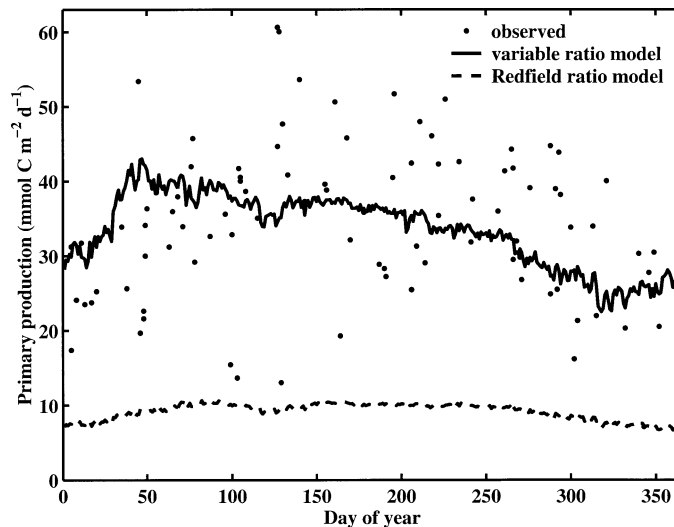


Fig. 7. Seasonal cycle of observed and modeled depth-integrated primary production at Station ALOHA.

the ocean (Winn et al. 1994; Dore et al. 2003; Quay and Stutsman 2003).

The air–sea flux in the model is generally less than data-based estimates (Table 4) largely due to the larger outgassing in summer. The net air–sea flux in the VRM is much larger than in the CRM; in fact, the mean flux in the CRM is out of the ocean when atmospheric  $\text{CO}_2$  is fixed at 1988 values (Table 4). This result may be exaggerated by the one-dimensional model framework, but it illustrates that the flux estimates are very sensitive to the ecosystem model formulation, and very close to zero in the CRM. The two models

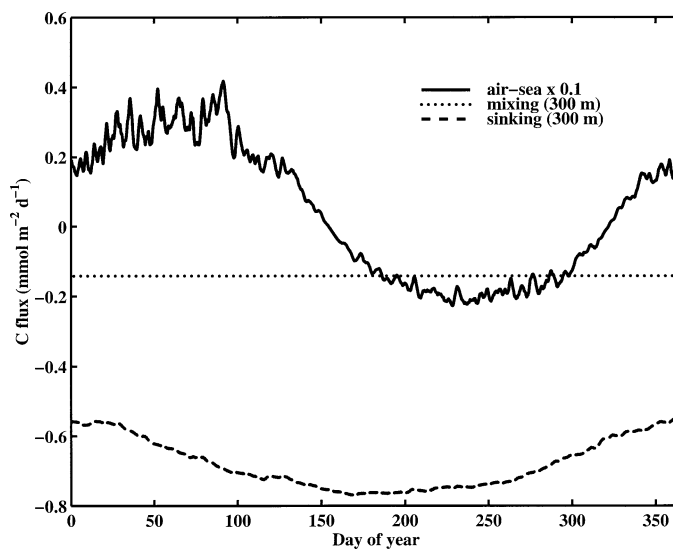


Fig. 8. Seasonal cycle of vertical fluxes of carbon: Sedimentation, mixing of DOC across the 300-m depth horizon, and air–sea exchange (scale compressed 10 times). Signs indicate gain or loss from upper ocean, i.e., positive air–sea flux is into ocean. Final year of 12-yr simulation with climatological forcing. Model output was low-pass filtered (2-d running mean) to smooth out high-frequency (e.g., diel) fluctuations.

Table 4. Summary of carbon flux estimates (in  $\text{mmol m}^{-2} \text{d}^{-1}$ ): primary production (PP), net community production (NCP), export by sedimentation of particulate organic carbon and by mixing of dissolved organic carbon (DOC), and air–sea flux of  $\text{CO}_2$  (positive into ocean).  $\text{NCP} = (\text{total uptake of DIC}) - (\text{total remineralization of all forms of organic carbon})$ . Sources for observed values: E97 = Emerson et al., 1997; K96 = Karl et al., 1996; QS03 = Quay and Stutsman, 2003. Climatology runs are the mean of final year of 12-yr simulation; interannual runs are means for 1989–2000; climatology uses 1988 atmospheric  $\text{CO}_2$ . Model export estimates are at 150 m; PP and NCP are integrated to 150 m. E97 estimates of the mixing flux of DOC are at 100 m; K96 sinking flux is at 150 m; QS93 NCP is for the surface mixed layer only.

Model	Forcing	PP	NCP	Export sinking	Export mixing	Air–sea flux
CRM*	Climatology	11.0	1.4	1.0	0.76	–0.32
	Interannual	11.1	1.5	1.0	0.77	0.12
	Interannual + 1988 a $\text{CO}_2$					–0.24
VRM	Climatology	36.1	2.7	1.2	0.82	0.44
	Interannual	40.4	2.9	1.3	0.91	1.05
	Interannual + 1988 a $\text{CO}_2$					0.68
Observed Source		38.6 K96	7.0 QS03	2.4 K96	2.4 E97	2.1 QS03

\* CRM, constant ratio model; VRM, variable ratio model.

cannot be distinguished on the basis of comparisons of modeled and observed  $f\text{CO}_2$ . The mean seasonal cycle of  $f\text{CO}_2$  and air–sea flux is very similar in the two models, and the small but consistent offset between them is necessary to give a net air–sea flux (Fig. 9).

The downward flux of reduced carbon is lower than observationally based estimates (Karl et al. 1996; Emerson et al. 1997; Benitez-Nelson et al. 2001) and larger in the VRM than in the CRM (Table 4). The downward flux due to mixing of DOC is 70–80% of the sedimentation flux at 150 m (Table 4) but attenuates much more rapidly with depth. At 300 m the ratio of particulate to dissolved export is 4–5 (Fig. 8). The enhancement of C export by vertical mixing of DOC

is consistent with the estimates of Emerson et al. (1997), but this result is very sensitive to the depth horizon considered. Similarly, the net community production (NCP) estimates of Quay and Stutsman (2003) are for the mixed layer only, and considerably larger than those from the model (Table 4). NCP is sensitive to choice of depth range because it is negative in the lower euphotic zone and below. A significant amount of mixed-layer NCP is remineralized within the euphotic zone.

The modeled sedimentation flux shows a maximum in summer (Fig. 8). The shallow depth of winter convection at ALOHA means that the flux depends primarily on the seasonal cycle of solar irradiance (Letelier et al. 2004) and nitrogen fixation (whereas at BATS there is a maximum in spring). Export is only loosely tied to primary production in a primarily regenerative ecosystem, and observed rates are largely uncorrelated, which is in part expected because of the different space/time scales of the methodologies. But the modeled export flux does not depend on the existence of wintertime convection and entrainment of nutrients, although primary production shows a slight enhancement in late winter (Fig. 7). Export may be more closely tied to primary production in the model than in nature (i.e., the export ratio is relatively invariant), but the mechanisms underlying an export flux decoupled from entrainment of new nutrients are resolved to first order, and depend in part on the decoupling of photosynthesis and cell growth in the VRM (Table 4).

## Discussion

*Parameter choices and fit to data*—The results shown above indicate that accurate simulation of the HOT data set is greatly facilitated by including flexible elemental ratios in the phytoplankton model and permitting decoupling of photosynthesis from growth. It is important to emphasize that the models were not tuned to emphasize the contrast. Originally, I attempted to tune each model to best reproduce the observations. Later, I attempted to harmonize the values of most of the parameters that are common to both models (e.g., remineralization rates for DOM). A base parameter set

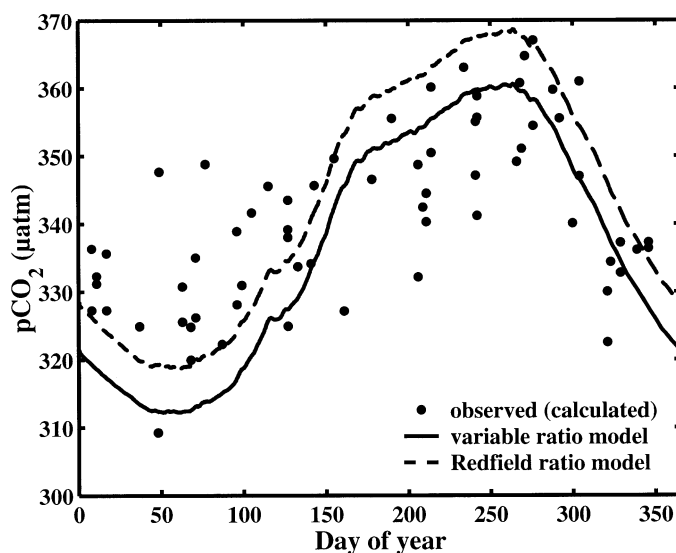


Fig. 9. Seasonal cycle of surface  $f\text{CO}_2$  at Station ALOHA in variable and Redfield ratio models. Final year of 12-yr simulation with climatological forcing. “Observed” values were calculated from measured DIC and alkalinity in identical fashion to modeled values for bottle samples at depths of 5 m or less. Model output was low-pass filtered (2-d running mean) to smooth out high-frequency (e.g., diel) fluctuations.

was defined for each model with as many common parameters as possible given a single value (Table 1), and simulated annealing (Press et al. 1992) was used to attempt to find a better fit to observations. The results of this experiment, in short, were that the value of the least-squares misfit function (based on dissolved organic and inorganic C, N, and P; chlorophyll; and oxygen) was about 100 times greater for the CRM than for the VRM, and that the parameter estimation algorithm did not narrow this gap much, even after thousands of iterations. Furthermore, the value of the misfit function for the VRM with its base parameter set was so low that the algorithm had little success in further reducing it, i.e., subjective tuning of the parameters produced something very close to the optimal solution for the eight fields chosen for the misfit function, but only in the VRM was this possible. The discrepancies between the two models are therefore real, i.e., they result from differences of model structure and not from parameter choices. A detailed account of the parameter estimation experiments and statistical analysis of the model parameter space is not possible here but will be given elsewhere.

Some unique attributes of the HOT data set make this model comparison possible. In particular, it is the only oceanographic program to have measured both organic and inorganic carbon, nitrogen, and phosphorus over an extended period of time, resolving complete seasonal cycles. It is possible, or even probable, that a RR model could adequately simulate a more limited set of observations. The most important discrepancy between the two models (and the major contributor to the least-squares misfit function) is the accumulation of DIN in near-surface waters in the CRM (Fig. 3). This is unlikely to occur in a nitrogen-only or nitrogen-carbon model, because N would be specified to be the limiting nutrient and would therefore be drawn down to about the level of the half-saturation coefficient. A hybrid model with C and N in RR and a flexible P quota (cf. Karl et al. 1992; Emerson et al. 2001) could potentially alleviate these problems, with a small gain in computation time over the full VRM.

Another important aspect of the HOT data set is the shallow depth of winter convection. At BATS, by contrast, nutrient entrainment by winter convection is the primary driver of the annual cycle of biological production, so its gross features are readily simulated by a fixed-ratio model (although rates of primary production in summer are likely to be underestimated). At HOT the annual cycle of primary production is controlled by irradiance and possibly by nitrogen fixation, and the model results strongly suggest that the photosynthesis measured by the  $^{14}\text{C}$  incubations is uncoupled from cell production (Figs. 6, 7). The VRM generates subsurface maxima in P-based production and to some degree in biomass (not shown); whether these are real or artificial is a question for future experiments since the quantities involved are not measured directly in the standard field protocols. The CRM generates a subsurface maximum even in C-based production, which is not observed (Fig. 6).

*Externalized processes*—There are several processes not considered in the model that have potential significance to the results, such as variability of zooplankton N:P ratios,

and control of DNF and DOM remineralization by, e.g., nutrient limitation. The present model parameterizes both the heterotrophic bacteria and the diazotrophic cyanobacteria so that rates of DNF and of remineralization are regulated in a very simple way by environmental conditions (light and temperature). Possible control of the biomass of these organisms by grazers, or their growth rates by nutrient limitation, are therefore excluded. There is also no export of diazotroph biomass; the only role of diazotrophs is to add new N that is then utilized by the other phytoplankton. The rate of remineralization of DOC is not limited by availability of N or P to heterotrophic bacteria.

It is possible that these processes may contribute to the observed variability, and therefore that their exclusion from the model may explain why it fails to capture much of that variability. However, it is unlikely that neglecting these processes would significantly alter the main results of this research. There are two ways in which it might do so. First, if diazotrophs were modeled explicitly, there might be sedimentation of material with elevated N:P that would limit the accumulation of DIN in the CRM (Fig. 3). However, this would further deplete the surface dissolved inorganic phosphorus pool, limiting uptake of DIN by nondiazotrophs and therefore the gain in model realism. More extreme N:P ratios in a large fraction of the particle flux are also inconsistent with some observations (Christian et al. 1997). Second, if remineralization of DOC were nutrient limited, the concentration of DOC in the CRM might remain higher and nearer the observed values (Fig. 5). However, evidence for nutrient limitation of DOC remineralization is weak, especially in oceanic waters (Carlson 2002). The ecosystem is a highly regenerative one: Although N and P concentrations are low, fluxes to the bacteria and cyanobacteria are high. In addition to facilitating DOC remineralization, rapid recycling of N and P is critical to sustaining the high observed rates of primary production, even in the VRM. Primary production is, furthermore, an example of a set of observations for which exclusion of these processes provides no plausible explanation of the discrepancy between the CRM and VRM.

A final process that has been neglected in the VRM is variability of zooplankton elemental ratios. If grazer N:P ratios differ significantly from those of the prey, the regenerated nutrient flux will have a characteristic N:P ratio that can drive the ecosystem toward N or P limitation (Sterner and Elser 2002). This phenomenon has been extensively documented in freshwater, but is not known to occur in the ocean. It is important to note that this is not a consequence of within-population variability of elemental ratios, but rather of taxonomic differences among species, each with ratios tightly regulated within set bounds (Sterner and Elser 2002). There is some evidence that the mean ratios for zooplankton may differ from the RR, although little is known about the micrograzers that dominate the primary grazer community in oceanic waters. I use the RR as a reference point in a study of variability about that reference point, which is strongly supported by observation as a mean value for the ecosystem as a whole, at least in the ocean (Sterner and Elser 2002).

*C:N:P stoichiometry and  $N_2$  fixation*—The model simulations show that the ecosystem is strongly N limited in the absence of DNF and strongly P limited given observed rates of DNF (Fig. 2). There are several areas of model-data disagreement that can not readily be resolved without postulating additional sources of P, such as low export (Table 4), and high surface DIC in summer, assuming that biological export is an important factor in removing this “excess” DIC (Quay and Stutsman 2003). There are several possible P sources or transport mechanisms that are unresolved by the model: Vertical migration of buoyancy-regulating cyanobacteria (Karl et al. 1992; Villareal and Carpenter 2003), upward fluxes of positively buoyant particulate P (Grimalt et al. 1990), mesoscale upwelling (Letelier et al. 2000), or large-scale convergence in the lateral advection of DOP (Abell et al. 2000). An additional possible “source” is that upper limits to C:P and N:P ratios, and therefore growth and export at very low concentrations of P, are larger than considered here.

While the P cell quota experiment (Table 2) suggests that further decreasing the minimum cell quota for nondiazotrophic phytoplankton would not enhance production and export, growth of diazotrophs at enhanced C:P and N:P ratios may explain some model-data discrepancies. In particular, the relatively low rates of export (Table 4) could be enhanced by growth and export of diazotrophs growing at high C:P ratios. This would be consistent with the results of Scharek et al. (1999), who showed large export in summer of diatoms with diazotrophic endosymbionts, and of Quay and Stutsman (2003), who observed an increase in  $\delta^{13}C$  of DIC in summer that implies enhanced biological uptake and export. This may imply that both symbiotic and free-living diazotrophic cyanobacteria (e.g., *Trichodesmium*) play important roles in C-N-P stoichiometry at ALOHA: the former in a highly seasonal pulse of export of material with very anomalous elemental ratios, the latter in alleviating N limitation throughout the year.

Further increasing C:P ratios in the phytoplankton generally is not a solution, because modeled values are already very high, approaching the upper limits in cultured *Prochlorococcus* and *Synechococcus* observed by Bertilsson et al. (2003). These authors speculated that in the ocean elemental ratios would not reach the extreme values observed in culture, and observed that phytoplankton ratios must be reconciled with those in bulk particulate matter, which generally approximates the RR. The modeled particle fluxes illustrate that the contribution of heterotroph biomass can explain this apparent paradox as suggested by Bertilsson et al. (2003), even without an explicit population of heterotrophic bacteria. Although the model does not include a suspended matter pool to directly compare with observations, the processes that give rise to the “virtual” sinking flux of particulate organic matter (POM) are the same as those that would generate suspended (nonliving) POM if the model had an explicit POM pool, and its elemental composition will be the same.

C:N:P ratios in the sinking flux at 300 m are generally near RR (Table 3); closer, in fact, than is indicated by the HOT sediment trap data (Christian et al. 1997). Possible explanations for this are (1) that heterotrophs (which have fixed

elemental ratios in the model) contribute to the vertical flux, and (2) that some of the flux originates in the deeper part of the euphotic zone where phytoplankton ratios are close to, or in the case of N:P less than, the RR. The model does not favor either autotrophs or heterotrophs in loss processes other than grazing: Both groups are removed at identical rates, which are proportional to biomass concentration. Nor does the model contain any mechanism by which organic matter originating at greater depths can be selectively exported. Yet the model, using a simple and plausible set of assumptions, resolves the apparent paradox of particle flux occurring near RR even when primary production deviates from it significantly. The key assumptions are that loss processes such as viral lysis do not selectively target autotrophs, and that remineralization of the sinking flux is not confined to the dysphotic zone, i.e., the flux of material originating at a particular depth horizon attenuates exponentially beginning at the point of origin (Web Appendix 1). Another important assumption is that excess C can be lost (exuded) from cells rapidly under conditions of unbalanced growth; however, there is no similar loss mechanism for N for which exudation occurs only at a low, constant biomass-specific rate (Bjørnsen 1988).

The “background” rate of DNF, attributable to *Trichodesmium* and free-living cyanobacteria and heterotrophic bacteria (Zehr et al. 2001), does not necessarily require additional inputs of P to sustain. The model implicitly assumes that DNF is not limited by availability of P or Fe, which is reasonable given the plasticity of N:P ratios (Karl et al. 1992). It is assumed that P export associated with the “background” DNF is negligible so that there is a net input of N to the pelagic ecosystem and no net loss of P. If these assumptions are correct, and summer diatom blooms (not resolved by the model) are also not limited by P sources (again due to biochemical plasticity), then elemental budgets can be largely balanced with known sources of P. However, the ecosystem as a whole is strongly P-limited, and the observed level of export approaches the upper limit that can be sustained by known sources of P to the epipelagic.

*Role of DOM and constraints on DOM remineralization*—Most of the DOM produced in the ocean is rapidly respired, whereas most of the DOM in the ocean is quite refractory to decomposition (Benner 2002). Bacteria respire a large fraction of the total primary production unless growth efficiency is much higher than currently believed (Ducklow 1999). So clearly a large fraction of primary production enters the pool of DOM that is rapidly turned over. The uncoupling of photosynthesis and cell production in the cellular regulation model provides an explanation for several apparent paradoxes. First is distribution of primary production at Station ALOHA. The distance between the region of maximal primary production and the pool of inorganic nutrients is large, and both the depth profile and the seasonal time course of primary production track the ambient solar irradiance closely as if nutrient supply were a secondary consideration (Figs. 6, 7). The VRM reproduces these vertical and seasonal patterns; the CRM does not. Second, the reconciliation of primary production, bacterial production, and growth efficiency estimates (Ducklow 1999) implies that la-

labile DOM is being produced in large quantities and rapidly consumed. The reconciliation of primary and bacterial production is also facilitated if existing estimates of primary production largely exclude the exuded fraction (Karl et al. 1998). The VRM, given the environmental conditions at ALOHA, generates a large excess of photosynthesis over cell production, which must be exuded and rapidly respired to satisfy other data constraints (C:N:P ratios in POM, ambient DOC and DIC concentrations). Nor is exudation the only source for labile DOM in the model. The DOM produced by lysis and grazing seems to be about evenly divided between the labile and semilabile fractions (Table 1), although it is important to recognize that this value cannot be constrained independently of the turnover rates of these pools.

Some of the labile DOM is likely to be transformed by bacteria into more refractory substances (Benner 2002 and references therein). This process has been included in some models (e.g., Bissett et al. 1999), but the underlying mechanisms are not known (Benner 2002; Carlson 2002). It has not been considered here because a large range of rates are compatible with the data constraints available and cannot be estimated independently of the other processes that generate semilabile DOM. However, some semilabile DOM likely originates from bacterial transformation of labile DOM, and this will affect the stoichiometry, for example by enriching semilabile DOM with C. The results of these model experiments suggest that exudation plays an important role in the production of DOC and in the decoupling of the C, N, and P cycles, but it is uncertain whether a significant fraction of semilabile and refractory DOM is of direct algal origin.

In conclusion, this experiment tested three-element (C, N, P) ecosystem models with fixed or variable phytoplankton elemental ratios, using the Hawaii Ocean Time-series data set. The results suggest that the ecosystem is strongly phosphorus limited, but would be nitrogen limited in the absence of DNF, and may be N limited in the lower part of the euphotic zone. Given observed rates of DNF, the fixed (Redfield) ratio model experiences accumulation of DIN in the surface layer. This would not happen in an N-only or C-N model, and validation on observations of N pools only is therefore an inadequate test of a fixed-ratio model. The seasonal cycles of air-sea CO<sub>2</sub> flux and export of organic carbon by sedimentation are similar in the two models, but there is a small but persistent bias toward greater downward fluxes with variable ratios. The ability of oceanic phytoplankton to adapt to P stress by reducing cellular requirements can therefore potentially enhance the oceanic sink for atmospheric carbon over vast areas of low-latitude ocean, but this effect is potentially saturable under a climate favorable to enhanced DNF. In the fixed-ratio model this area of the ocean is a weak sink for anthropogenic CO<sub>2</sub>, but becomes a carbon source to the atmosphere when atmospheric CO<sub>2</sub> is fixed at 1988 levels. The modulation of phytoplankton elemental ratios by environmental conditions is therefore a critical component of the ocean biological carbon sink.

## References

- ABELL, J., S. EMERSON, AND P. RENAUD. 2000. Distributions of TOP, TON, and TOC in the North Pacific subtropical gyre: Implications for nutrient supply in the surface ocean and remineralization in the upper thermocline. *J. Mar. Res.* **58**: 203–222.
- BAKER, A. R., S. D. KELLY, K. F. BISWAS, M. WITT, AND T. D. JICKELLS. 2003. Atmospheric deposition of nutrients to the Atlantic Ocean. *Geophys. Res. Lett.* **30**. [doi:10.1029/2003GL018518]
- BENITEZ-NELSON, B., K. O. BUESSELER, D. M. KARL, AND J. ANDREWS. 2001. A time-series study of particulate matter export in the North Pacific Subtropical Gyre based on <sup>234</sup>Th:<sup>238</sup>U disequilibrium. *Deep-Sea Res.* **48**: 2595–2611.
- BENNER, R. 2002. Chemical composition and reactivity, p. 59–90. *In* D. A. Hansell and C. A. Carlson [eds.], *Biogeochemistry of marine dissolved organic matter*. Academic.
- BERTILSSON, S., O. BERGLUND, D. M. KARL, AND S. W. CHISHOLM. 2003. Elemental composition of marine *Prochlorococcus* and *Synechococcus*: Implications for the ecological stoichiometry of the sea. *Limnol. Oceanogr.* **48**: 1721–1731.
- BISHOP, J. K. B., W. B. ROSSOW, AND E. G. DUTTON. 1997. Surface solar irradiance from the International Satellite Cloud Climatology Project. *J. Geophys. Res.* **102**: 6883–6910.
- BISSETT, W. P., J. J. WALSH, D. A. DIETERLE, AND K. L. CORDER. 1999. Carbon cycling in the upper waters of the Sargasso Sea: I. Numerical simulation of differential carbon and nitrogen fluxes. *Deep-Sea Res.* **46**: 205–269.
- BJØRNSSEN, P. K. 1988. Phytoplankton exudation of organic matter: Why do healthy cells do it? *Limnol. Oceanogr.* **33**: 151–154.
- CARLSON, C. A. 2002. Production and removal processes, p. 91–151. *In* D. A. Hansell and C. A. Carlson [eds.], *Biogeochemistry of marine dissolved organic matter*. Academic.
- CHRISTIAN, J. R., AND T. A. ANDERSON. 2002. Modeling DOM biogeochemistry, p. 717–755. *In* D. A. Hansell and C. A. Carlson [eds.], *Biogeochemistry of marine dissolved organic matter*. Academic.
- , M. R. LEWIS, AND D. M. KARL. 1997. Vertical fluxes of carbon, nitrogen, and phosphorus in the North Pacific Subtropical Gyre near Hawaii. *J. Geophys. Res.* **102**: 15667–15677.
- CORNELL, S., A. RENDELL, AND T. JICKELLS. 1995. Atmospheric inputs of dissolved organic nitrogen to the oceans. *Nature* **376**: 243–246.
- DORE, J. E., R. LUKAS, D. W. SADLER, AND D. M. KARL. 2003. Climate-driven changes to the atmospheric CO<sub>2</sub> sink in the subtropical North Pacific Ocean. *Nature* **424**: 754–757.
- DUCKLOW, H. W. 1999. The bacterial component of the oceanic euphotic zone. *FEMS Microbiol. Ecol.* **30**: 1–10.
- EMERSON, S., S. MECKING, AND J. ABELL. 2001. The biological pump in the subtropical North Pacific Ocean: Nutrient sources, Redfield ratios, and recent changes. *Global Biogeochem. Cycles* **15**: 535–554.
- , P. QUAY, D. KARL, C. WINN, L. TUPAS, AND M. LANDRY. 1997. Experimental determination of the organic carbon flux from open-ocean surface waters. *Nature* **389**: 951–954.
- FOGG, G. E. 1983. The ecological significance of extracellular products of phytoplankton photosynthesis. *Bot. Mar.* **26**: 3–14.
- GEIDER, R. J., H. L. MACINTYRE, AND T. M. KANA. 1998. A dynamic regulatory model of phytoplankton acclimation to light, nutrients, and temperature. *Limnol. Oceanogr.* **43**: 679–694.
- GILL, A. E. 1982. *Atmosphere-ocean dynamics*. Academic.
- GOLDMAN, J. C., J. J. MCCARTHY, AND D. G. PEAVEY. 1979. Growth rate influence on the chemical composition of phytoplankton in oceanic waters. *Nature* **279**: 210–215.
- GRIMALT, J. O., B. R. T. SIMONEIT, J. I. GOMEZ-BELINCHON, K. FISCHER, AND J. DYMOND. 1990. Ascending and descending fluxes of lipid compounds in North Atlantic and North Pacific abyssal waters. *Nature* **345**: 147–150.

- HUFFMAN, G. J., AND OTHERS. 1997. The Global Precipitation Climatology Project (GPCP) combined precipitation dataset. *Bull. Am. Meteorol. Soc.* **78**: 5–20.
- KALNAY, E., AND OTHERS. 1996. The NCEP/NCAR 40-year reanalysis project. *Bull. Am. Meteorol. Soc.* **77**: 437–471.
- KARL, D. M., AND OTHERS. 2001a. Ecological nitrogen-to-phosphorus stoichiometry at Station ALOHA. *Deep-Sea Res. II* **48**: 1529–1566.
- , J. R. CHRISTIAN, J. E. DORE, D. V. HEBEL, R. M. LETELIER, L. M. TUPAS, AND C. D. WINN. 1996. Seasonal and interannual variability in primary production and particle flux at Station ALOHA. *Deep-Sea Res. II* **43**: 539–568.
- , J. E. DORE, R. LUKAS, A. F. MICHAELS, N. R. BATES, AND A. KNAP. 2001b. Building the long-term picture: The US-JGOFS time-series programs. *Oceanogr. Mag.* **14**: 6–17.
- , D. V. HEBEL, K. BJORKMAN, AND R. M. LETELIER. 1998. The role of dissolved organic matter exudation in the productivity of the oligotrophic North Pacific Ocean. *Limnol. Oceanogr.* **43**: 1270–1286.
- , R. LETELIER, D. V. HEBEL, D. F. BIRD, AND C. D. WINN. 1992. *Trichodesmium* blooms and new nitrogen in the north Pacific gyre, p. 219–237. In E. J. Carpenter, D. G. Capone, and J. G. Reuter [eds.], *Marine pelagic cyanobacteria: Trichodesmium and other diazotrophs*. Kluwer.
- , ———, L. M. TUPAS, J. E. DORE, J. R. CHRISTIAN, AND D. V. HEBEL. 1997. The role of nitrogen fixation in biogeochemical cycling in the subtropical North Pacific ocean. *Nature* **388**: 533–538.
- KEELING, C. D., R. B. BACASTOW, A. E. BAINBRIDGE, C. A. EKDAHL, P. R. GUENTHER, L. S. WATERMAN, AND J. F. S. CHIN. 1976. Atmospheric carbon dioxide variations at Mauna Loa Observatory, Hawaii. *Tellus* **28**: 538–551.
- KIRK, J. T. O. 1994. *Light and photosynthesis in aquatic ecosystems*. Cambridge Univ. Press.
- LETELIER, R. M., D. M. KARL, M. R. ABBOTT, AND R. R. BIDIGARE. 2004. Light driven seasonal patterns of chlorophyll and nitrate in the lower euphotic zone of the North Pacific Subtropical Gyre. *Limnol. Oceanogr.* **49**: 508–519.
- , ———, ———, P. FLAMENT, M. FREILICH, R. LUKAS, AND T. STRUB. 2000. Role of late winter mesoscale events in the biogeochemical variability of the North Pacific subtropical gyre. *J. Geophys. Res.* **105**: 28723–28739.
- PRESS, W. H., S. A. TEUKOLSKY, W. T. VETTERLING, AND B. P. FLANNERY. 1992. *Numerical recipes in FORTRAN*. Cambridge Univ. Press.
- PRICE, J. F., R. E. WELLER, AND R. PINKEL. 1986. Diurnal cycling: Observations and models of the upper ocean response to diurnal heating, cooling, and wind mixing. *J. Geophys. Res.* **91**: 8411–8427.
- QUAY, P., AND J. STUTSMAN. 2003. Surface layer carbon budget for the subtropical N. Pacific:  $\delta^{13}\text{C}$  constraints at station ALOHA. *Deep-Sea Res. I* **50**: 1045–1061.
- REDFIELD, A. C., B. H. KETCHUM, AND F. A. RICHARDS. 1963. The influence of organisms on the composition of sea-water, p. 26–77. In M. N. Hill [ed.], *The sea*. Wiley.
- SCHAREK, R., M. LATASA, D. M. KARL, AND R. R. BIDIGARE. 1999. Temporal variations in diatom abundance and downward vertical flux in the oligotrophic North Pacific gyre. *Deep-Sea Res. I* **46**: 1051–1075.
- SIGNORINI, S. R., C. R. MCCLAIN, J. R. CHRISTIAN, AND C. S. WONG. 2001. Seasonal and interannual variability of phytoplankton, nutrients,  $\text{TCO}_2$ ,  $\text{pCO}_2$ , and  $\text{O}_2$  in the eastern subarctic Pacific (ocean weather station Papa). *J. Geophys. Res.* **106**: 31197–31215.
- STERNER, R. W., AND J. J. ELSER. 2002. *Ecological stoichiometry: The biology of elements from molecules to the biosphere*. Princeton Univ. Press.
- TERRY, K. L., E. A. LAWS, AND D. J. BURNS. 1985. Growth rate variation in the N:P requirement ratio of phytoplankton. *J. Phycol.* **21**: 323–329.
- VILLAREAL, T. A., AND E. J. CARPENTER. 2003. Buoyancy regulation and the potential for vertical migration in the oceanic cyanobacterium *Trichodesmium*. *Microb. Ecol.* **45**: 1–10.
- WANNINKHOF, R. 1992. Relationship between wind speed and gas exchange over the ocean. *J. Geophys. Res.* **97**: 7373–7382.
- WEISS, R. F. 1970. The solubility of nitrogen, oxygen, and argon in water and seawater. *Deep-Sea Res.* **17**: 721–735.
- . 1974. Carbon dioxide in water and seawater: The solubility of a non-ideal gas. *Mar. Chem.* **2**: 203–215.
- , AND B. A. PRICE. 1980. Nitrous oxide solubility in water and seawater. *Mar. Chem.* **8**: 347–359.
- WINN, C. D., F. T. MACKENZIE, C. J. CARRILLO, C. L. SABINE, AND D. M. KARL. 1994. Air-sea carbon dioxide exchange in the North Pacific subtropical gyre: Implications for the global carbon budget. *Global Biogeochem. Cycles* **8**: 157–163.
- ZEHR, J. P., AND OTHERS. 2001. Unicellular cyanobacteria fix  $\text{N}_2$  in the subtropical North Pacific Ocean. *Nature* **412**: 635–638.

Received: 19 May 2004

Accepted: 25 October 2004

Amended: 17 November 2004